The Astrophysical Journal Letters, 882:L13 (6pp), 2019 September 1 https://doi.org/10.3847/2041-8213/ab3c5f

Limits on the Weak Equivalence Principle and Photon Mass with FRB 121102 Subpulses

Nan Xing[1], He Gao[1], Jun-Jie Wei[2], Zhengxiang Li[1], Weiyang Wang[3,4], Bing Zhang[5], Xue-Feng Wu[2], and Peter Mészáros[6,7,8]
[1] Department of Astronomy, Beijing Normal University, Beijing 100875, People's Republic of China; gaohe@bnu.edu.cn
[2] Purple Mountain Observatory, Chinese Academy of Sciences, Nanjing 210008, People's Republic of China
[3] Key Laboratory for Computational Astrophysics, National Astronomical Observatories, Chinese Academy of Sciences, 20A Datun Road, Beijing 100101, People's Republic of China
[4] University of Chinese Academy of Sciences, Beijing 100049, People's Republic of China
[5] Department of Physics and Astronomy, University of Nevada Las Vegas, Las Vegas, NV 89154, USA
[6] Department of Astronomy and Astrophysics, Pennsylvania State University, 525 Davey Laboratory, University Park, PA 16802, USA
[7] Department of Physics, Pennsylvania State University, 104 Davey Laboratory, University Park, PA 16802, USA
[8] Center for Particle and Gravitational Astrophysics, Institute for Gravitation and the Cosmos, Pennsylvania State University, 525 Davey Laboratory, University Park, PA 16802, USA
Received 2019 July 15; revised 2019 August 14; accepted 2019 August 16; published 2019 September 3

Abstract

Fast radio bursts (FRBs) are short-duration (∼millisecond) radio transients with cosmological origin. The simple sharp features of the FRB signal have been utilized to probe two fundamental laws of physics, namely, testing Einstein's weak equivalence principle and constraining the rest mass of the photon. Recently, Hessels et al. found that after correcting for dispersive delay, some of the bursts in FRB 121102 have complex time–frequency structures that include subpulses with a time–frequency downward drifting property. Using the delay time between subpulses in FRB 121102, here we show that the parameterized post-Newtonian parameter γ is the same for photons with different energies to the level of $|\gamma_1 - \gamma_2| < 2.5 \times 10^{-16}$, which is 1000 times better than previous constraints from FRBs using similar methods. We also obtain a stringent constraint on the photon mass, $m_\gamma < 5.1 \times 10^{-48}$ g, which is 10 times smaller than previous best limits on the photon mass derived through the velocity dispersion method.

Unified Astronomy Thesaurus concepts: Radio transient sources (2008)

1. Introduction

Fast radio bursts (FRBs) are short-duration radio transients with anomalously high dispersion measure in excess of the Galactic value (DM $\gtrsim 200$ pc cm^{-3}; Lorimer et al. 2007; Keane et al. 2012; Thornton et al. 2013; Petroff et al. 2016). The first repeating burst FRB 121102 was localized in a star-forming dwarf galaxy at $z = 0.193$, which has confirmed the cosmological origin of FRBs (Scholz et al. 2016; Spitler et al. 2016; Chatterjee et al. 2017; Marcote et al. 2017; Tendulkar et al. 2017). Recently, two nonrepeating FRBs were precisely localized. The first one is FRB 180924, which was localized in a luminous and massive galaxy at redshift 0.3214 by the Australia Square Kilometre Array Pathfinder (Bannister et al. 2019). The other one is FRB 190523, which was localized with the Deep Synoptic Array 10-antenna prototype to a massive galaxy at redshift 0.66 (Ravi et al. 2019).

Although the progenitors and radiation mechanism are still debated, FRBs have been proposed to be promising tools for cosmological and astrophysical studies, such as locating the "missing" baryons (Mcquinn 2014), constraining the cosmological parameters (Gao et al. 2014; Zhou et al. 2014; Yang & Zhang 2016a; Walters et al. 2018), directly measuring Ω_b of the universe (Deng & Zhang 2014; Keane et al. 2016), probing the reionization history of the universe (Deng & Zhang 2014; Zheng et al. 2014; Caleb et al. 2019; Li et al. 2019), probing compact dark matter or precisely measuring the Lemaître–Hubble–Humason constant and the cosmic curvature through gravitationally lensed FRBs (Muñoz et al. 2016; Laha 2018a; Li et al. 2018; Wang & Wang 2018), measuring cosmic proper distances (Yu & Wang 2017), testing Einstein's weak equivalence principle (WEP; Wei et al. 2015; Nusser 2016; Tingay & Kaplan 2016; Wu et al. 2017; Yu et al. 2018), and constraining the rest mass of the photon (Bonetti et al. 2016, 2017; Wu et al. 2016b; Shao & Zhang 2017).

FRB emission arrives later at lower radio frequencies. In principle, the observed time delay for a cosmic transient between two different energy bands should include various terms (Gao et al. 2015; Wei et al. 2015), such as the intrinsic (astrophysical) time delay $\Delta t_{\rm int}$, which means photons with different energies were emitted sequentially due to the dynamical process or radiation mechanism, the time delay contribution from the dispersion by the line-of-sight free electron content $\Delta t_{\rm DM}$, the potential time delay caused by special relativistic effects ($\Delta t_{\rm spe}$) in the case where the photons have a rest mass that is nonzero, and the potential time delay caused by the violation of Einstein's WEP ($\Delta t_{\rm gra}$) where photons with different energies follow different trajectories while traveling in the same gravitational potential.[9] In FRB observations, the arrival time delay $\Delta t_{\rm obs}$ is around 1 s and at a given frequency ν follows a ν^{-2} law (Lorimer et al. 2007; Keane et al. 2012; Thornton et al. 2013; Petroff et al. 2016). This is compatible with both plasma and massive photon dispersion (de Broglie 1940). The time delay is routinely attributed to plasma, but there is not an independent, that is, by other means, confirmation that such an attribution is entirely correct.

In this case, a conservative constraint on the WEP can be obtained under the assumption that $\Delta t_{\rm obs}$ is mainly contributed by $\Delta t_{\rm gra}$. Using FRB 110220 and two possible FRB/gamma-ray burst (GRB) association systems (FRB/GRB 101011A and FRB/GRB

[9] In principle, gravitational fields associated with $\Delta t_{\rm gra}$ should include contributions from the host galaxy potential, the intergalactic potential, and the local gravitational potential. In practice, for the purposes of obtaining a lower limit, here we only consider the local potential contribution. See Section 2 for a detailed discussion.

100704A), Wei et al. (2015) obtained a strict upper limit on the differences of the parameterized post-Newtonian (PPN) parameter γ values, e.g., $|\gamma(1.23\ \mathrm{GHz}) - \gamma(1.45\ \mathrm{GHz})| < 4.36 \times 10^{-9}$. Keane et al. (2016) reported the connection between a fading radio transient with FRB 150418, so that a putative host galaxy with redshift 0.492 ± 0.008 was identified (see counter opinions in Williams & Berger 2016, where the counterpart radio transient is claimed to be active galactic nucleus variability instead of an afterglow of FRB 150418). Assuming that 0.492 is the redshift of FRB 150418, Tingay & Kaplan (2016) and Nusser (2016) obtained more stringent upper limits on the differences of γ values as (1–2) $\times 10^{-9}$ and 10^{-12}–10^{-13} by considering the Milky Way (MW) and the large-scale structure gravitational potential, respectively.

On the other hand, if one assumes that $\Delta t_{\rm obs}$ of an FRB is mainly contributed by $\Delta t_{\rm spe}$, a conservative limit on the rest mass of the photon could be placed. For instance, taking $z = 0.492$ as the redshift of FRB 150418, a conservative upper limit for the rest mass of the photon was placed as $m_{\rm ph} \leqslant 5.2 \times 10^{-47}$ g, which is 10^{20} times smaller than the rest mass of the electron (Bonetti et al. 2016; Wu et al. 2016b). Later, Bonetti et al. (2017) applied a similar method to FRB 121102, and they obtained a similar result as $m_{\rm ph} \leqslant 3.6 \times 10^{-47}$ g.

Most recently, Hessels et al. (2019) found that some bursts in FRB 121102 have complex time–frequency structures that include subbursts with finite bandwidths. After correcting for dispersive delay, the subbursts still show an interesting subpulse time–frequency downward drifting pattern, namely, the characteristic frequencies for subpulses drift lower at later times in the total burst envelope. The same features are also found in the second discovered repeating FRB source, FRB 180814.J0422+73 (CHIME/FRB Collaboration et al. 2019). Such features could be intrinsic (e.g., related to the burst emission mechanism; Wang et al. 2019), or they could also be imparted by propagation effects (Cordes et al. 2017; Hessels et al. 2019). Plasma lensing may cause upward and downward subpulse drifts, but only downward drifting is observed so far in the repeating FRBs. In the 1.1–1.7 GHz band, the typical time spans for subpulses are ~0.5–1 ms, with a characteristic drift rate of ~200 MHz ms^{-1} toward lower frequencies.[10] Considering that FRB 121102 is the only FRB with confirmed redshift observations, and the time delay between subpulses is almost 10^4 times smaller than the dispersive delay, it is of great interest to place limits on the WEP and the photon mass with the FRB 121102 subpulses.

2. Testing the Einstein Weak Equivalence Principle

The Einstein WEP is an important foundation of many metric theories of gravity, including general relativity. One statement of the WEP is that test particles traveling in the same gravitational potential will follow the same trajectory, regardless of their internal structure and composition (Will 2006). Therefore, it has long been proposed that the accuracy of the WEP can be constrained with the time delay for different types of messenger particles (e.g., photons, neutrinos, or gravitational waves), or the same types of particles but with different energies or different polarization states, which are simultaneously radiated from the same astronomical sources.

According to the Shapiro time delay effect (Shapiro 1964), the time interval required for test particles to traverse a given distance would be longer by

$$t_{\rm gra} = -\frac{1+\gamma}{c^3}\int_{r_e}^{r_o} U(r)dr, \tag{1}$$

in the presence of a gravitational potential $U(r)$, where the test particles are emitted at r_e and received at r_o. Here γ is one of the PPN parameters, which reflects how much space curvature is produced by unit rest mass. When the WEP is invalid, different particles might correspond to different γ values. In this case, two particles emitted simultaneously from the source will arrive at the Earth with a time delay difference

$$\Delta t_{\rm gra} = \frac{\gamma_1 - \gamma_2}{c^3}\int_{r_o}^{r_e} U(r)dr, \tag{2}$$

where γ_1 and γ_2 correspond to two different test particles. For a cosmic source, in principle, $U(r)$ has contributions from the host galaxy potential $U_{\rm host}(r)$, the intergalactic potential $U_{\rm IG}(r)$, and the local gravitational potential $U_{\rm local}(r)$. Since the potential models for $U_{\rm IG}(r)$ and $U_{\rm host}(r)$ are poorly known, for the purposes of obtaining a lower limit, it is reasonable to extend the local potential out to cosmic scales to bracket from below the potential function of $U_{\rm IG}(r)$ and $U_{\rm host}(r)$. In the previous works, the gravitational potential of the MW or the Laniakea supercluster (Tully et al. 2014) has been used as the local potential, which could be expressed as a Keplerian potential[11] $U(r) = -{\rm GM}/r$. In this case, we have

$$\Delta t_{\rm gra} = (\gamma_1 - \gamma_2)\frac{GM}{c^3}\times \ln\left\{\frac{[d + (d^2 - b^2)^{1/2}][r_L + s_{\rm n}(r_L^2 - b^2)^{1/2}]}{b^2}\right\}, \tag{3}$$

where d is the distance from the transient to the MW/Laniakea center and b is the impact parameter of the light rays relative to the center. Here we use $s_{\rm n} = +1$ or $s_{\rm n} = -1$ to denote the cases where the transient is located along the direction of the MW/Laniakea or anti-MW/Laniakea center. For a cosmic source, d is approximated as the distance from the source to the Earth. The impact parameter can be estimated as

$$b = r_L\sqrt{1 - (\sin\delta_s \sin\delta_L + \cos\delta_s \cos\delta_L \cos(\beta_s - \beta_L))^2}\ , \tag{4}$$

where β_s and δ_s are the source coordinates, β_L and δ_L represent the coordinates of the local (MW/Laniakea) center, and r_L is the distance from the Earth to the center.

In the literature, many investigations have been done to achieve stringent limits on γ differences between particles emitted from the same astrophysical sources, such as supernovae 1987A (Krauss & Tremaine 1988; Longo 1988), GRBs (Gao et al. 2015; Wei et al. 2016b; Wu et al. 2017; Yang et al. 2017; Wei & Wu 2019), FRBs

[10] With 3.5 yr of weekly observations of PSR J2219+4754, Donner et al. (2019) present the first detection of frequency-dependent, time-variable dispersion measures. It is worth noticing that the typical timescale for the time variability proposed by Donner et al. (2019) is several days, much longer than the FRB duration, so that it cannot be used to explain the observed subpulse structures of FRBs.

[11] Although the potential models for the Laniakea supercluster are still not well known, it has been tested that the adoption of the Keplerian potential model, compared with other widely used potential model, i.e., the isothermal potential would not have a strong influence on the results for testing the WEP (Krauss & Tremaine 1988).

(Wei et al. 2015; Nusser 2016; Tingay & Kaplan 2016; Wu et al. 2017), blazars (Wang et al. 2016; Wei et al. 2016a, 2019), the Crab pulsar (Yang & Zhang 2016b; Zhang & Gong 2017), and gravitational-wave (GW) sources (Kahya & Desai 2016; Wu et al. 2016a; Abbott et al. 2017; Wei et al. 2017a; Shoemaker & Murase 2018). The previous results are summarized in Table 1. When the test particles are of different species, the best constraint is $|\gamma_1 - \gamma_2| < 1.3 \times 10^{-13}$ for keV photons and the TeV neutrino from GRB 110521B (Wei et al. 2016b). When the test particles are the same species but with different energies, the best constraint is $|\gamma_1 - \gamma_2| < (0.6 - 1.8) \times 10^{-15}$ for 8.15–10.35 GHz photons from the Crab pulsar (Yang & Zhang 2016b). When the test particles are of the same species but with different polarization states, the best constraint is $|\gamma_1 - \gamma_2| < 0.8 \times 10^{-33}$ for polarized gamma-ray photons from GRB 061122 (Wei & Wu 2019).

Here we considered the time–frequency structure of FRB 121102. As shown in Hessels et al. (2019), after correcting for dispersive delay, several subpulses still exist in some of the FRB 121102 repeated bursts. Each subpulse corresponds to its own characteristic frequency, and subpulses with higher frequencies arrive earlier. Assuming that these subpulses are emitted simultaneously and the observed time delay is mainly caused by the WEP effect, a stringent limit on the WEP can be placed by using the time delay between any two subpulses. In order to get more stringent constraints, here we consider the closest neighboring subpulses in AO-05, where the time delay between $f_1 = 1374.16$ MHz and $f_2 = 1343.69$ MHz is 0.4 ms. With the inferred coordinates and redshifts for FRB 121102 (here we adopt R.A. $= \beta_s = 05^{\rm h}32^{\rm m}$, decl. $= \delta_{\rm s} = +33°08'$ and $z = 0.193$; Spitler et al. 2016), we obtain

$$|\gamma_1 - \gamma_2| < 2.5 \times 10^{-16}, \quad (5)$$

where we consider the gravitational potential of the Laniakea supercluster as the local potential, the Great Attractor ($\beta_L = 10^{\rm h}32^{\rm m}$, $\delta_L = -46°00'$) is adopted as the gravitational center of Laniakea (Lynden-Bell et al. 1988), $M_{\rm L} \simeq 10^{17} M_\odot$ is the Laniakea mass, and $r_L = 79$ Mpc is the distance from the Earth to the center of Laniakea (Tully et al. 2014). The result is 1000 times better than previous constraints from FRBs and 4 times better than previous best constraints for the case when the test particles are of the same species but with different energies. It is worth noticing that the uncertainty of the adopted gravitational potential would affect the constraints. Conservatively, we can consider the Keplerian potential for the MW, where the impact parameter can be estimated as $b = r_G \sqrt{1 - (\sin\delta_s \sin\delta_G + \cos\delta_s \cos\delta_G \cos(\beta_s - \beta_G))^2}$, where $r_G = 8.3$ kpc is the distance from the Earth to the Galaxy center, and ($\beta_G = 17^{\rm h}45^{\rm m}40\overset{\rm s}{.}04$, $\delta_G = -29°00'28\overset{''}{.}1$) are the coordinates of the Galaxy center in the equatorial coordinate system (J2000; Gillessen et al. 2009). In this case, we have

$$|\gamma_1 - \gamma_2| < 9.6 \times 10^{-12}, \quad (6)$$

where the Galaxy mass is adopted as $M = 6 \times 10^{11} M_\odot$ (Kafle et al. 2012).

3. Constraints on the Photon Mass

The postulate that all electromagnetic radiation propagates in vacuum at the constant speed c, namely, that the photons should have a zero rest mass, is one of the most important foundations of Einstein's theory of special relativity. If the photon mass is nonzero, a mass term should be added to the Lagrangian density for the electromagnetic field to describe the effective range of the electromagnetic interaction (de Broglie 1923, 1940; Proca 1936). In this case, some abnormal phenomena will appear for the electromagnetic potentials and their derivatives, for instance, the speed of light is no longer constant but depends on the frequency of the photons, magnetic dipole fields would decrease with distance very rapidly due to the addition of a Yukawa component, longitudinal electromagnetic waves could exist, and so on. Such effects could be applied to make restrictive constraints on the photon rest mass (Goldhaber & Nieto 1971, 2010; Tu et al. 2005; Pani et al. 2012). The current limit on the photon mass accepted by the Particle Data Group (PDG) is from the solar wind observation (Tanabashi et al. 2018), which is set to $m_\gamma \leqslant 1.5 \times 10^{-51}$ g (but see Retinò et al. 2016 for comments and an experiment in the solar wind referring to the PDG upper limit).

It has long been proposed that the photon rest mass could be constrained by using the frequency-dependent time delays of multiwavelength emissions from astrophysical sources (Lovell et al. 1964; Warner & Nather 1969; Schaefer 1999; Bonetti et al. 2016, 2017; Wu et al. 2016b; Shao & Zhang 2017; Wei et al. 2017b; Wei & Wu 2018). According to Einstein's special relativity, if the photon has a rest mass m_γ, the photon energy can be written as

$$E = h\nu = \sqrt{p^2c^2 + m_\gamma^2 c^4}, \quad (7)$$

where h is the Planck constant. In vacuum, the speed of photons with energy E can be derived as

$$v = \frac{\partial E}{\partial p}. \quad (8)$$

When $m_\gamma = 0$, we have $v = c$. If $m_\gamma \neq 0$, we have

$$v = \frac{\partial E}{\partial p} = c\sqrt{1 - \frac{m_\gamma^2 c^4}{E^2}} \approx c\left(1 - \frac{1}{2}\frac{m_\gamma^2 c^4}{h^2\nu^2}\right), \quad (9)$$

where the last approximation is applicable when $m_\gamma \ll h\nu/c^2 \simeq 7 \times 10^{-39}\left(\frac{\nu}{\rm GHz}\right)$ g. In this case, two photons with different frequencies, which are emitted simultaneously from the same source, would arrive on the Earth at different times with a time–frequency downward drifting pattern. For a cosmic source, the arrival time difference is given by

$$\Delta t_{m_\gamma} = \frac{m_\gamma^2 c^4}{2h^2 H_0}(\nu_l^{-2} - \nu_h^{-2}) \int_0^z \frac{(1+z')^{-2} dz'}{\sqrt{\Omega_{\rm m}(1+z')^3 + \Omega_\Lambda}}, \quad (10)$$

where H_0 is the Lemaître–Hubble–Humason constant (Lemaître 1927; Hubble 1929; Hubble & Humason 1931). Thus, the photon mass can be constrained as (Wu et al. 2016b)

$$m_\gamma = (1.56 \times 10^{-47}{\rm g})\left[\frac{H_{70}\Delta t_{m_\gamma}}{(\nu_{l,9}^{-2} - \nu_{h,9}^{-2}) \int_0^z \frac{(1+z')^{-2} dz'}{\sqrt{\Omega_{\rm m}(1+z')^3 + \Omega_\Lambda}}}\right]^{1/2}, \quad (11)$$

where ν_9 is the radio frequency in units of 10^9 Hz and H_{70} is the Lemaître–Hubble–Humason constant in units of 70 km s^{-1} Mpc^{-1}.

Table 1
Upper Limits on the Differences of the γ Values through the Shapiro Time Delay Effect

Categorization	Author (year)	Source	Messengers	Gravitational Field	$\Delta\gamma$
Same particles with different energies	This work	FRB 121102	1.374–1.344 GHz photons	Laniakea supercluster of galaxies	2.5×10^{-16}
	Wei et al. (2015)	FRB 110220	1.2–1.5 GHz photons	Milky Way	2.5×10^{-8}
		FRB/GRB 100704A	1.23–1.45 GHz photons	Milky Way	4.4×10^{-9}
	Tingay & Kaplan (2016)	FRB 150418	1.2–1.5 GHz photons	Milky Way	$(1–2) \times 10^{-9}$
	Nusser (2016)	FRB 150418	1.2–1.5 GHz photons	Large-scale structure	10^{-12}–10^{-13}
	Longo (1988)	SN 1987A	7.5–40 MeV neutrinos	Milky Way	1.6×10^{-6}
	Gao et al. (2015)	GRB 090510	MeV–GeV photons	Milky Way	2.0×10^{-8}
		GRB 080319B	eV–MeV photons	Milky Way	1.2×10^{-7}
	Yang & Zhang (2016b)	Crab pulsar	8.15–10.35 GHz photons	Milky Way	$(0.6–1.8) \times 10^{-15}$
	Desai & Kahya (2018)	Crab pulsar	8.15–10.35 GHz photons	Milky Way	2.4×10^{-15}
	Zhang & Gong (2017)	Crab pulsar	eV–MeV photons	Milky Way	3.0×10^{-10}
	Leung et al. (2018)	Crab pulsar	1.52–2.12 eV photons	Milky Way	1.1×10^{-10}
	Wei et al. (2016a)	Mrk 421	keV–TeV photons	Milky Way	3.9×10^{-3}
		PKS 2155-304	sub TeV–TeV photons	Milky Way	2.2×10^{-6}
	Wu et al. (2016a)	GW150914	35–150 Hz GW signals	Milky Way	$\sim 10^{-9}$
	Kahya & Desai (2016)	GW150914	35–250 Hz GW signals	Milky Way	2.6×10^{-9}
Different particles	Krauss & Tremaine (1988)	SN 1987A	eV photons and MeV neutrinos	Milky Way	5.0×10^{-3}
	Longo (1988)	SN 1987A	eV photons and MeV neutrinos	Milky Way	3.4×10^{-3}
	Wei et al. (2016b)	GRB 110521B	keV photons and TeV neutrino	Laniakea supercluster of galaxies	1.3×10^{-13}
	Wang et al. (2016)	PKS B1424-418	MeV photons and PeV neutrino	Virgo Cluster	3.4×10^{-4}
		PKS B1424-418	MeV photons and PeV neutrino	Great Attractor	7.0×10^{-6}
	Boran et al. (2019)	TXS 0506+056	GeV photons and TeV neutrino	Milky Way	5.5×10^{-2}
	Laha (2018b); Wei et al. (2019)	TXS 0506+056	GeV photons and TeV neutrino	Laniakea supercluster of galaxies	10^{-6}–10^{-7}
	Wei et al. (2017a)	GW170817	MeV photons and GW signals	Virgo Cluster	9.2×10^{-11}
		GW170817	eV photons and GW signals	Virgo Cluster	2.1×10^{-6}
	Abbott et al. (2017)	GW170817	MeV photons and GW signals	Milky Way	-2.6×10^{-7}–1.2×10^{-6}
	Shoemaker & Murase (2018)	GW170817	MeV photons and GW signals	Milky Way	7.4×10^{-8}
	Boran et al. (2018)	GW170817	MeV photons and GW signals	Milky Way	9.8×10^{-8}
Same particles with different polarization states	Wu et al. (2017)	GRB 120308A	Polarized optical photons	Laniakea supercluster of galaxies	1.2×10^{-10}
		GRB 100826A	Polarized gamma-ray photons	Laniakea supercluster of galaxies	1.2×10^{-10}
		FRB 150807	Polarized radio photons	Laniakea supercluster of galaxies	2.2×10^{-16}
	Yang et al. (2017)	GRB 110721A	Polarized gamma-ray photons	Milky Way	1.6×10^{-27}
	Wei & Wu (2019)	GRB 061122	Polarized gamma-ray photons	Laniakea supercluster of galaxies	0.8×10^{-33}
		GRB 110721A	Polarized gamma-ray photons	Laniakea supercluster of galaxies	1.3×10^{-33}

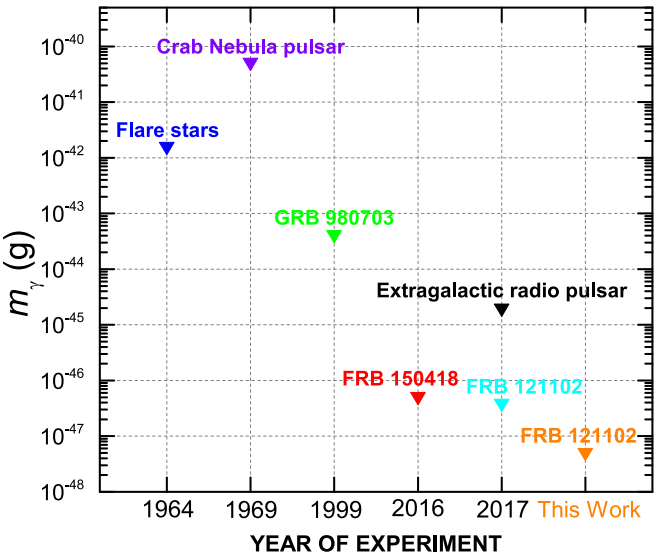

Figure 1. Strict upper limits on the photon rest mass from the velocity dispersion method, including the upper limits from flare stars (Lovell et al. 1964), Crab Nebula pulsar (Warner & Nather 1969), GRB 980703 (Schaefer 1999), extragalactic radio pulsars (Wei et al. 2017b), FRB 150418 (Bonetti et al. 2016; Wu et al. 2016b), FRB 121102 (Bonetti et al. 2017), and FRB 121102 subpulses.

In the literature, many attempts have been made to obtain constraints on the photon rest mass by considering various astrophysical sources, including flare stars (Lovell et al. 1964), the Crab Nebula pulsar (Warner & Nather 1969), FRBs (Bonetti et al. 2016, 2017; Wu et al. 2016b; Shao & Zhang 2017), GRBs (Schaefer 1999), and pulsars in the Large and Small Magellanic Clouds (Wei et al. 2017b; Wei & Wu 2018). The constraint results are shown in Figure 1. The current best constraint on the photon mass through the velocity dispersion method is made by using the radio emissions from FRB 121102, $m_\gamma \leqslant 3.6 \times 10^{-47}$ g (Bonetti et al. 2017), where the time delay between the whole observational bandwidth is considered, and $\Delta t_{\rm obs}$ is on the order of 1 s.

Here we propose to use the observed time delay between subpulses in FRB 121102 to obtain more stringent constraints on the photon mass, by assuming that the time delay between subpulses is mainly due to the massive photon effect, which is reasonable since the subpulses with lower frequencies arrive later. We adopt the closest neighboring subpulses in AO-05 ($\Delta t_{\rm obs} = 0.4$ ms between $f_1 = 1374.16$ MHz and $f_2 = 1343.69$ MHz) and obtain a stringent limit on the photon mass as $m_\gamma < 5.1 \times 10^{-48}$ g, where $z = 0.193$ is adopted for FRB 121102, and the Planck results are adopted for cosmological parameters, e.g., $H_0 = 67.8$ km s^{-1} Mpc^{-1}, $\Omega_m = 0.308$, and $\Omega_\Lambda = 0.692$ (Planck Collaboration et al. 2018).[12] Note that since the redshift of FRB 121102 is relatively small, the uncertainty of cosmological parameters would not affect the constraints too much. For instance, when H_0 varies from 67.8 to 73.2 km s^{-1} Mpc^{-1} (Riess et al. 2016), the limit on the photon mass varies from $m_\gamma < 5.1 \times 10^{-48}$ g to $m_\gamma < 5.3 \times 10^{-48}$ g. When the value of Ω_m varies from 0.2 to 0.4 (Ω_Λ thus varies from 0.8 to 0.6), the limit on the photon mass varies from $m_\gamma < 5.0 \times 10^{-48}$ g to $m_\gamma < 5.1 \times 10^{-48}$g.

As shown in Figure 1, our result is 10 times better than that obtained using other FRB sources, and $\sim 10^4$ times better than that obtained by GRBs, $\sim 10^3$ times better than that obtained by pulsars in the Large and Small Magellanic Clouds, $\sim 10^6$ times better than flare stars, and $\sim 10^7$ times better than the Crab Nebula pulsar.

4. Discussion

Using the time–frequency structure of subpulses in some bursts of FRB 121102, here we have obtained a stringent limit on the γ differences between photons with different energies of $|\gamma_1 - \gamma_2| < 2.5 \times 10^{-16}$, which is 1000 times better than previous constraints from FRBs through similar methods. In addition, we also obtained a stringent constraint on the photon mass of $m_\gamma < 5.1 \times 10^{-48}$ g, which is 10 times better than the previous best limits on the photon mass using the velocity dispersion method.

It is worth stressing the advantages of the method for placing limits on the WEP and the photon mass using the time–frequency structure of the subpulses of, e.g., FRB 121102. In previous works, the time delay between the whole observational bandwidth of FRBs (on the order of 1 s) were applied to make constraints on the WEP or the photon mass. Such a time delay at a given frequency ν follows a ν^{-2} law, which is compatible with both plasma and massive photon dispersion. Considering that the column density of free electrons inferred from the time delay is roughly consistent with the theoretical predictions (accumulated contributions from MK, IGM, and host galaxy; Chatterjee et al. 2017), the time delay is routinely attributed to plasma, although without an independent confirmation that such attribution is entirely correct. The time–frequency structure of the FRB 121102 subpulses, however, emerges after correcting for dispersive delays. Therefore, the time delay between subpulses is largely reduced to the order of milliseconds or even submilliseconds, which is very advantageous for further improving the accuracy of a basic physical analysis. Moreover, it has been proposed that the observed downward drifting of the subpulse frequency is more likely intrinsic, namely, a generic geometrical effect within the framework of coherent curvature radiation by bunches of electron–positron pairs in the magnetosphere of a neutron star (Wang et al. 2019). If this is the case, the constraints on the WEP and the photon mass would become even tighter.

This work is supported by the National Natural Science Foundation of China (NSFC) under grant Nos. 11690024, 11722324, 11603003, 11633001, 11725314, 11603076, U1831122; the Strategic Priority Research Program of the Chinese Academy of Sciences, grant No. XDB23040100; and the Fundamental Research Funds for the Central Universities. W.Y.W. acknowledges the support from MoST grant 2016YFE0100300; NSFC under grant Nos. 11633004, 11473044, 11653003; and the CAS grant QYZDJ-SSW-SLH017. P.M. acknowledges the Eberly Foundation.

ORCID iDs

He Gao https://orcid.org/0000-0002-3100-6558
Peter Mészáros https://orcid.org/0000-0002-4132-1746

[12] The extra subpulse delay in the de-dispersed profile may appear to suggest that the subpulse delay does not satisfy the ν^{-2} law predicted by massive photon dispersion. However, Hessels et al. (2019) showed that the subpulse structure appears only when the DM is chosen to maximize the burst profile. For other trial DMs, the substructure would disappear, which suggests that the subpulses in those cases follow the ν^{-2} law but with a smaller separation. Our adoption of a larger separation therefore gives a more conservative constraint on the mass of photon.

References

Abbott, B. P., Abbott, R., Abbott, T. D., et al. 2017, ApJL, 848, L13
Bannister, K. W., Deller, A. T., Phillips, C., et al. 2019, arXiv:1906.11476
Bonetti, L., Ellis, J., Mavromatos, N. E., et al. 2016, PhLB, 757, 548
Bonetti, L., Ellis, J., Mavromatos, N. E., et al. 2017, PhLB, 768, 326
Boran, S., Desai, S., Kahya, E. O., et al. 2018, PhRvD, 97, 041501
Boran, S., Desai, S., & Kahya, E. O. 2019, EPJC, 79, 185
Caleb, M., Flynn, C., & Stappers, B. W. 2019, MNRAS, 485, 2281
Chatterjee, S., Law, C. J., Wharton, R. S., et al. 2017, Natur, 54, 58
CHIME/FRB Collaboration, Amiri, M., Bandura, K., et al. 2019, Natur, 566, 235
Cordes, J. M., Wasserman, I., Hessels, J. W. T., et al. 2017, ApJ, 842, 35
de Broglie, L. 1923, Comptes Rendus Hebd. Séances Acad. Sc. Paris, 177, 507
de Broglie, L. 1940, La Mécanique Ondulatoire du Photon. Une Nouvelle Théorie de la Lumière (Paris: Hermann et cie)
Deng, W., & Zhang, B. 2014, ApJL, 783, L35
Desai, S., & Kahya, E. 2018, EPJC, 78, 86
Donner, J. Y., Verbiest, J. P. W., Tiburzi, C., et al. 2019, A&A, 624, A22
Gao, H., Li, Z., & Zhang, B. 2014, ApJ, 788, 189
Gao, H., Wu, X.-F., & Mészáros, P. 2015, ApJ, 810, 121
Gillessen, S., Eisenhauer, F., Trippe, S., et al. 2009, ApJ, 692, 1075
Goldhaber, A. S., & Nieto, M. M. 1971, RvMP, 43, 277
Goldhaber, A. S., & Nieto, M. M. 2010, RvMP, 82, 939
Hessels, J. W. T., Spitler, L. G., Seymour, A. D., et al. 2019, ApJL, 876, L23
Hubble, E. 1929, PNAS, 15, 168
Hubble, R., & Humason, M. L. 1931, ApJ, 74, 43
Kafle, P. R., Sharma, S., Lewis, G. F., & Bland-Hawthorn, J. 2012, ApJ, 761, 98
Kahya, E. O., & Desai, S. 2016, PhLB, 756, 265
Keane, E. F., Johnston, S., Bhandari, S., et al. 2016, Natur, 530, 453
Keane, E. F., Stappers, B. W., Kramer, M., & Lyne, A. G. 2012, MNRAS, 425, L71
Krauss, L. M., & Tremaine, S. 1988, PhRvL, 60, 176
Laha, R. 2018a, arXiv:1812.11810
Laha, R. 2018b, arXiv:1807.05621
Lemaître, G. 1927, Ann. Soc. Sci. Bruxelles A, 47, 49
Leung, C., Hu, B., Harris, S., et al. 2018, ApJ, 861, 66
Li, Z., Gao, H., Ding, X., Wang, G., & Zhang, B. 2018, NatCo, 9, 3833
Li, Z., Gao, H., Wei, J.-J., et al. 2019, ApJ, 876, 146
Longo, M. J. 1988, PhRvL, 60, 173
Lorimer, D. R., Bailes, M., McLaughlin, M. A., Narkevic, D. J., & Crawford, F. 2007, Sci, 318, 777
Lovell, B., Whipple, F. L., & Solomon, L. H. 1964, Natur, 202, 377
Lynden-Bell, D., Faber, S. M., Burstein, D., et al. 1988, ApJ, 326, 19
Marcote, B., Paragi, Z., Hessels, J. W. T., et al. 2017, ApJL, 834, L8
Mcquinn, M. 2014, ApJL, 780, L33
Muñoz, J. B., Kovetz, E. D., Dai, L., & Kamionkowski, M. 2016, PhRvL, 117, 091301
Nusser, A. 2016, ApJL, 821, L2
Pani, P., Cardoso, V., Gualtieri, L., Berti, E., & Ishibashi, A. 2012, PhRvL, 109, 131102
Petroff, E., Barr, E. D., Jameson, A., et al. 2016, PASA, 33, e045
Planck Collaboration, Aghanim, N., Akrami, Y., et al. 2018, arXiv:1807.06209
Proca, A. 1936, J. Phys. Radium, 7, 347
Ravi, V., Catha, M., Daddario, L., et al. 2019, arXiv:1907.01542
Retinò, A., Spallicci, A. D. A. M., & Vaivads, A. 2016, APh, 82, 49
Riess, A. G., Macri, L. M., Hoffmann, S. L., et al. 2016, ApJ, 826, 56
Schaefer, B. E. 1999, PhRvL, 82, 4964
Scholz, P., Spitler, L. G., Hessels, J. W. T., et al. 2016, ApJ, 833, 177
Shao, L., & Zhang, B. 2017, PhRvD, 95, 123010
Shapiro, I. I. 1964, PhRvL, 13, 789
Shoemaker, I. M., & Murase, K. 2018, PhRvD, 97, 083013
Spitler, L. G., Scholz, P., Hessels, J. W. T., et al. 2016, Natur, 531, 202
Tanabashi, M., Hagiwara, K., Hikasa, K., et al. 2018, PhRvD, 98, 030001
Tendulkar, S. P., Bassa, C. G., Cordes, J. M., et al. 2017, ApJL, 834, L7
Thornton, D., Stappers, B., Bailes, M., et al. 2013, Sci, 341, 53
Tingay, S. J., & Kaplan, D. L. 2016, ApJL, 820, L31
Tu, L.-C., Luo, J., & Gillies, G. T. 2005, RPPh, 68, 77
Tully, R. B., Courtois, H., Hoffman, Y., et al. 2014, Natur, 513, 71
Walters, A., Weltman, A., Gaensler, B. M., et al. 2018, ApJ, 856, 65
Wang, W., Zhang, B., Chen, X., et al. 2019, ApJL, 876, L15
Wang, Y. K., & Wang, F. Y. 2018, A&A, 614, A50
Wang, Z.-Y., Liu, R.-Y., & Wang, X.-Y. 2016, PhRvL, 116, 151101
Warner, B., & Nather, R. E. 1969, Natur, 222, 157
Wei, J.-J., Gao, H., Wu, X.-F., et al. 2015, PhRvL, 115, 261101
Wei, J.-J., Wang, J.-S., Gao, H., et al. 2016a, ApJL, 818, L2
Wei, J.-J., & Wu, X.-F. 2018, JCAP, 2018, 045
Wei, J.-J., & Wu, X.-F. 2019, PhRvD, 99, 103012
Wei, J.-J., Wu, X.-F., Gao, H., et al. 2016b, JCAP, 2016, 031
Wei, J.-J., Zhang, B.-B., Shao, L., et al. 2019, JHEAp, 22, 1
Wei, J.-J., Zhang, B.-B., Wu, X.-F., et al. 2017a, JCAP, 11, 035
Wei, J.-J., Zhang, E.-K., Zhang, S.-B., & Wu, X.-F. 2017b, RAA, 17, 13
Will, C. M. 2006, LRR, 9, 3
Williams, P. K. G., & Berger, E. 2016, ApJL, 821, L22
Wu, X.-F., Gao, H., Wei, J.-J., et al. 2016a, PhRvD, 94, 024061
Wu, X.-F., Wei, J.-J., Lan, M.-X., et al. 2017, PhRvD, 95, 103004
Wu, X.-F., Zhang, S.-B., Gao, H., et al. 2016b, ApJL, 822, L15
Yang, C., Zou, Y.-C., Zhang, Y.-Y., Liao, B., & Lei, W.-H. 2017, MNRAS, 469, L36
Yang, Y.-P., & Zhang, B. 2016a, ApJL, 830, L31
Yang, Y.-P., & Zhang, B. 2016b, PhRvD, 94, 101501
Yu, H., & Wang, F. Y. 2017, A&A, 606, A3
Yu, H., Xi, S.-Q., & Wang, F.-Y. 2018, ApJ, 860, 173
Zhang, Y., & Gong, B. 2017, ApJ, 837, 134
Zheng, Z., Ofek, E. O., Kulkarni, S. R., Neill, J. D., & Juric, M. 2014, ApJ, 797, 71
Zhou, B., Li, X., Wang, T., Fan, Y.-Z., & Wei, D.-M. 2014, PhRvD, 89, 107303